EXTENDED VERSION OF ARTICLE FROM:
DINAME 2019 - Proceedings of the XVIII International Symposium on Dynamic Problems of Mechanics,
M.A. Savi, T.G. Ritto and W.M. Bessa (Editors), ABCM, Buzios, RJ, Brazil, March 10th to 15th, 2019

Angular Position Control of Furuta Pendulum with an Intelligent Sliding Modes Approach

Diego Rolim Porto[1], **Gabriel da Silva Lima**[1], **and Wallace Moreira Bessa**[1]

[1] Manufacturing Laboratory, Mechanical Engineering Dept., Center of Technology, Federal University of Rio Grande do Norte, Natal, Brazil.

Abstract: Underactuated mechanical systems have several applications in the industrial activity. With that in mind, the study of controllers suitable for these type of mechanisms is vital. In this article, a controller composed of the combination of the sliding mode and artificial neural networks techniques is proposed. Being tested on a Furuta pendulum, with a highly nonlinear dynamic and uncertainties, the results clearly show a great improvement in the overall performance.

Keywords: Underactuated mechanical systems, sliding mode control, artificial neural network

INTRODUCTION

For fully actuated systems, characterized for having the same number of actuator and degrees of freedom, the usage of traditional control methodologies, such as, feedback linearization (Slotine and Li, 1991) and sliding modes control (Ashrafiuon and Erwin, 2008), have been shown effective for these type of systems.

However, in underactuated systems, with less actuator than degrees of freedom, the conventional methods cited above are challenged due to the high number of uncertainties and the dynamic complexity associated with the system (Bessa and Kreuzer, 2018). Thus, in the last years, the development of control techniques for highly uncertain and nonlinear systems received more attention. Mainly, the usage of adaptive or intelligent techniques, as well as, modification of already proven and highly used control methods (Farrel and Polycarpou, 2006).

Also, should be taken into account the determining factor that are responsible for underactuation. Seifried (2013) expose three factors, design errors, non rigid or unmodeled dynamics and actuator failure. These factor render evident the necessity of the study and development of controllers capable of tackling such situations and risks. In addition, advancement in the field allows the designer to completely neglect some uncertainties, such as, friction and model parameters, reduction of energy cost with removal of actuators and viability of certain mechanisms for practical industrial usage, such as cranes and quadrotors.

Intelligent control has been proved to be effective to deal with nonlinear systems (Bessa and Barrêto, 2010; Bessa et al., 2012; Tanaka et al., 2013). Therefore, the idea of combining artificial neural networks (ANN) and a sliding modes controller (SMC) to cope with unmodeled external influences and lack of parameters precision, respectively, is very appealing and proposed by this article.

METHODOLOGY

Mathematical Equations

Utilizing lagrangian mechanics to obtain the movement equations of mechanical systems, it is possible to write these equations for a given mechanism, with n degrees of freedom and m actuators, in the following matrix form (Seifried, 2013):

$$\boldsymbol{M}(\boldsymbol{q})\ddot{\boldsymbol{q}} + \boldsymbol{k}(\boldsymbol{q},\dot{\boldsymbol{q}}) = \boldsymbol{g}(\boldsymbol{q},\dot{\boldsymbol{q}}) + \boldsymbol{B}(\boldsymbol{q})\boldsymbol{u} \tag{1}$$

where $\boldsymbol{q} \in \mathbb{R}^n$ is vector of generalized coordinates, $\boldsymbol{u} \in \mathbb{R}^m$ is the actuator gain vector, $\boldsymbol{M}(\boldsymbol{q}) \in \mathbb{R}^{nxn}$ is the inertia matrix, positive and symmetric, $\boldsymbol{k}(\boldsymbol{q},\dot{\boldsymbol{q}}) \in \mathbb{R}^n$ represents the influence of centrifugal forces and Coriolis, $\boldsymbol{g}(\boldsymbol{q},\dot{\boldsymbol{q}}) \in \mathbb{R}^n$ is the vector of external forces applied in the system and $\boldsymbol{B}(\boldsymbol{q}) \in \mathbb{R}^{nxm}$ is the input vector.

With the objective of simplifying the aplication of the control technique, the Eq.(1) can be reorganized in a new form, where the actuated and underactuated variables, $\boldsymbol{q}_a$ and $\boldsymbol{q}_u$ respectively, are separated and the effect of centrifugal, Coriolis and generalized forces are merged in a single term. (Ashrafiuon and Erwin, 2008; Seifried and Blajer, 2013).

$$\begin{bmatrix} \boldsymbol{M}_{aa} & \boldsymbol{M}_{au} \\ \boldsymbol{M}_{ua} & \boldsymbol{M}_{uu} \end{bmatrix} \begin{bmatrix} \ddot{\boldsymbol{q}}_a \\ \ddot{\boldsymbol{q}}_u \end{bmatrix} = \begin{bmatrix} \boldsymbol{f}_a + \boldsymbol{u} \\ \boldsymbol{f}_u \end{bmatrix} \tag{2}$$

where $\boldsymbol{f}_a = \boldsymbol{g}_a - \boldsymbol{k}_a$ and $\boldsymbol{f}_u = \boldsymbol{g}_u - \boldsymbol{k}_u$.

Control Methodology

The control law acting in the system should be capable of ensuring that the vector of generalized coordinates, $\boldsymbol{q}$, will follow the desired trajectory, $\boldsymbol{q}^d$. Defining the variable $\tilde{\boldsymbol{q}} = \boldsymbol{q} - \boldsymbol{q}^d$ as the tracking error vector, the necessary conditions defined above can be rewritten as: $\tilde{\boldsymbol{q}} \to 0$ as $t \to \infty$.

Considering, in the application, the sliding modes control methodology. It is necessary to define the sliding surfaces for each actuated coordinate of the system. Thus, for $\boldsymbol{s} \in \mathbb{R}^m$ in the state space, is defined:

$$\begin{aligned} \boldsymbol{s}(\tilde{\boldsymbol{q}}) &= \alpha_a \dot{\tilde{\boldsymbol{q}}}_a + \lambda_a \tilde{\boldsymbol{q}}_a + \alpha_u \dot{\tilde{\boldsymbol{q}}}_u + \lambda_u \tilde{\boldsymbol{q}}_u = 0 \\ &= \alpha_a \dot{\boldsymbol{q}}_a + \alpha_u \dot{\boldsymbol{q}}_u + \boldsymbol{s}_r = 0 \end{aligned} \tag{3}$$

where $\boldsymbol{s}_r = -\alpha_a \dot{\boldsymbol{q}}_a^d - \alpha_u \dot{\boldsymbol{q}}_u^d + \lambda_a \tilde{\boldsymbol{q}}_a + \lambda_u \tilde{\boldsymbol{q}}_u$.

Consequently, the sliding modes controller must satisfy the candidate Lyapunov function and the slidind condition, presented, respectively, in Eq.(4) and Eq.(5). Which, by definition, guarantee stability and convergence to the tracking error dynamic(Ashrafiuon and Erwin, 2008).

$$V(\boldsymbol{q}, \dot{\boldsymbol{q}}) = \frac{1}{2} \boldsymbol{s}^\top \boldsymbol{s} \tag{4}$$

$$\dot{V}(\boldsymbol{q}, \dot{\boldsymbol{q}}) \leq 0 \tag{5}$$

On this basis, the control law is defined as (Ashrafiuon and Erwin, 2008):

$$\boldsymbol{u} = -\hat{\boldsymbol{M}}_s^{-1} \left[\hat{\boldsymbol{f}}_s + \dot{\boldsymbol{s}}_r + \boldsymbol{\kappa} sgn(\boldsymbol{s}) \right] \tag{6}$$

where $\hat{\boldsymbol{M}}_s$ and $\hat{\boldsymbol{f}}_s$ are estimates of $\boldsymbol{M}_s$ and $\boldsymbol{f}_s$, matrices that represent the behavior of the real system. The controller gain, $\boldsymbol{\kappa}$, must be determined taking into account the model parameters errors, any unmodeled dynamics and external disturbances (Bessa and Kreuzer, 2018). For the control law described in Eq.(6) to work, the following assumptions are made. The error in the estimated variables are unknown but bounded, and the vector of generalized coordinates $\boldsymbol{q}$ and desired trajectory $\boldsymbol{q}^d$ are available.

However, the discontinuous term in Eq.(6), the signal function, creates a well known effect in the actuated variables, the chattering. A strategy to deal with these unwanted high-frequency oscillations is to substitute the signal function for a smooth approximation, defined in Eq.(7), nearby the switching surface. The substitution can reduce and, even, completely eliminate the chattering effect. But renders the controller incapacitated, in other words, there will always be a steady-state error.

$$sat(s_i/\phi_i) = \begin{cases} sgn(s_i) & if \quad |s_i/\phi_i| \geq 1 \\ s_i/\phi_i & if \quad |s_i/\phi_i| \leq 1 \end{cases} \tag{7}$$

where $\phi \in \mathbb{R}^{mxm}$ is the diagonal matrix defining the boundary layer, $sat(\cdot)$ is the saturation function and $\boldsymbol{\kappa}$ is defined according to $\kappa_i \geq \zeta + \delta_i + |\hat{d}_i|$ in order to ensure convergence.

The addition of the compensation term, $\hat{\boldsymbol{d}}_s$, based in an artificial neural networks, within the smoothed version of the control law shown in Eq.(6) is proposed.

$$\boldsymbol{u} = -\hat{\boldsymbol{M}}_s^{-1} \left[\hat{\boldsymbol{f}}_s + \hat{\boldsymbol{d}}_s + \dot{\boldsymbol{s}}_r + \boldsymbol{\kappa}\, sat(\boldsymbol{\phi}^{-1} \boldsymbol{s}) \right] \tag{8}$$

This compensator has the objective of handling the remaining errors and uncertainties, related to $\boldsymbol{d}_s$, inside the boundary layer created by the control law presented in Eq.(8). Assuming the form of a RBF neural network (Haykin, 2008), the approximation $\hat{\boldsymbol{d}}_s$ can be calculated by the Eq.(9).

$$\hat{d}_i(s_i) = \hat{\boldsymbol{W}}_i^\top \boldsymbol{\Psi}_i(s_i) \tag{9}$$

where $\hat{\boldsymbol{W}}_i = [\hat{w}_{i1} \dots \hat{w}_{iN}]^\top$ are vectors of weights of all N nodes and each sliding surface, $\boldsymbol{\Psi}_i(s_i) = [\psi_{i1}(s_i) \dots \psi_{iN}(s_i)]^\top$ are the activation function vectors, with ψ_{ij} being a gaussian function with determined center and width.

Assuming the existence of a vector of ideal weights $\bar{\boldsymbol{W}}$ that perfectly model $\boldsymbol{d}_s$, and following the procedure as developed in Bessa et al(2017), is defined a adaptation law that guarantees the best estimate. This is shown in Eq.(10).

$$\dot{\hat{\boldsymbol{W}}} = \eta_i s_i \boldsymbol{\Psi}_i(s_i) \tag{10}$$

where η is a positive constant associated to the learning rate.

APPLIED EXAMPLE

The system chosen to apply the proposed control law is the rotational inverted pendulum (Furuta), demonstrated in Fig. 1, with the following movement equation.

$$\begin{bmatrix} -I_1 - {l_1}^2 m_2 - \frac{{l_2}^2 m_2}{2} + \frac{1}{2}{l_2}^2 m_2 \cos(2\theta_2) & l_1 l_2 m_2 \cos(\theta_2) \\ l_1 l_2 m_2 \cos(\theta_2) & -I_2 - {l_2}^2 m_2 \end{bmatrix} \begin{bmatrix} \ddot{\theta}_1 \\ \ddot{\theta}_2 \end{bmatrix} + \begin{bmatrix} -l_2 m_2 \sin(\theta_2)\dot{\theta}_2(2 l_2 \cos(\theta_2)\dot{\theta}_1 + l_1 \dot{\theta}_2) \\ {l_2}^2 m_2 \cos(\theta_2)\sin(\theta_2)\dot{\theta}_1^2 \end{bmatrix} = \begin{bmatrix} 0 \\ l_2 m_2 \sin(\theta_2) g \end{bmatrix} + \begin{bmatrix} \tau \\ 0 \end{bmatrix} \tag{11}$$

where θ_j represent angular displacement, m_j is the mass associated with that element, with $j = 1,2;$, respectively representing the rotation base and the pendulum. I_1 is the inertia moment of the rotation base around the Z_1 axis, I_2 is the inertia moment of the pendulum around the Y_2 axis, l_1 is the radius of the rotation base, and l_2 is the length of the pendulum.

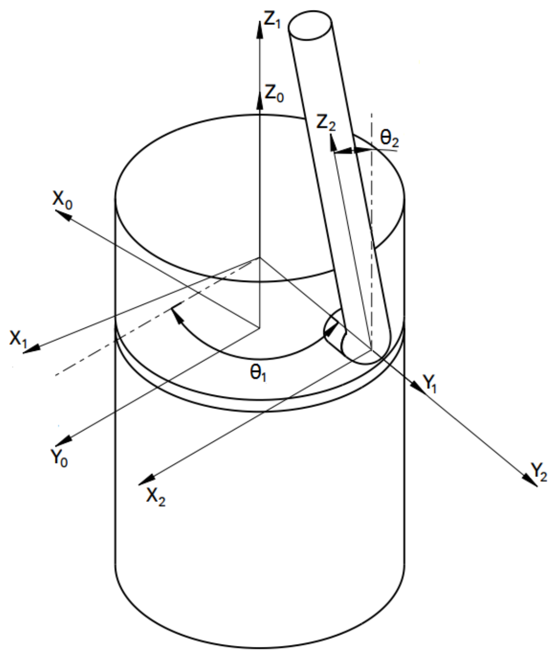

Figure 1: Representation of the system modeled

with the fact the only θ_1 can be directly controlled by the actuator. Following the proposed methodology by Ashrafiuon and Erwin (2008), the switching surface by $s = \alpha_a \dot{\tilde{\theta}}_1 + \lambda_a \tilde{\theta}_1 + \alpha_u \dot{\tilde{\theta}}_2 + \lambda_u \tilde{\theta}_2$, with $\tilde{\theta}_1 = \theta_1 - \theta_1^d$ and $\tilde{\theta}_2 = \theta_2 - \theta_2^d$ being the state errors. Then, with the inclusion of the compensation term that, in this case, have the objective to approximate the unmodeled dynamic of viscous damping, the control law is:

$$u = -\hat{M}_s \left[\hat{f}_s + \hat{d}_s + \dot{s}_r + \kappa sat(s/\phi)\right] \tag{12}$$

where κ is the control gain, ϕ is associated to the width of the boundary layer, $\dot{s}_r = -\alpha_a \ddot{\theta}_1^d - \alpha_u \ddot{\theta}_2^d + \lambda_a \dot{\tilde{\theta}}_1 + \lambda_u \dot{\tilde{\theta}}_2$, and

$$\hat{M}_s = \frac{-2(\alpha_a(A) + \alpha_u D)}{-2I_1(A) - m_2(I_2(2{l_1}^2 + {l_2}^2) + {l_2}^2 B) + C(I_2 + B)\cos(2\theta_2)}$$

$$\hat{f}_s = \frac{-E(2\alpha_a D + \alpha_u(2I_1 + 2{l_1}^2 + C - C\cos(2\theta_2)))(g + l_2\cos(\theta_2)\dot{\theta}_1{}^2)}{-2I_1(A) - m_2(I_2(2{l_1}^2 + {l_2}^2) + {l_2}^2 B) + C(I_2 + B)\cos(2\theta_2)} + \frac{E(4 l_2 \cos(\theta_2)(\alpha_a(A) + \alpha_u D)\dot{\theta}_1\dot{\theta}_2 + 2 l_1(\alpha_a(A + \alpha_u D)\dot{\theta}_2{}^2))}{-2I_1(A) - m_2(I_2(2{l_1}^2 + {l_2}^2) + {l_2}^2 B) + C(I_2 + B)\cos(2\theta_2)}$$

with $A = I_2 + {l_2}^2 m_2$, $B = ({l_1}^2 + {l_2}^2) m_2$, $C = {l_2}^2 m_2$, $D = l_1 l_2 m_2 \cos(\theta_2)$, $E = l_2 m_2 \sin(\theta_2)$.

Fig. 2(a) represents the artificial neural network architecture used to estimate the parameter $\hat{d}_s$ for the furuta pendulum. This neural network is composed by: seven nodes centered in $[-\phi/4 \;\; -\phi/20 \;\; -\phi/40 \;\; 0 \;\; \phi/40 \;\; \phi/20 \;\; \phi/4]^\top$ with the width vector being $[\psi/2 \;\; \psi/5 \;\; \psi/5 \;\; \psi/15 \;\; \psi/5 \;\; \psi/5 \;\; \psi/2]^\top$. The formed gaussian functions, using the control parameters, are shown in Fig. 2(b).

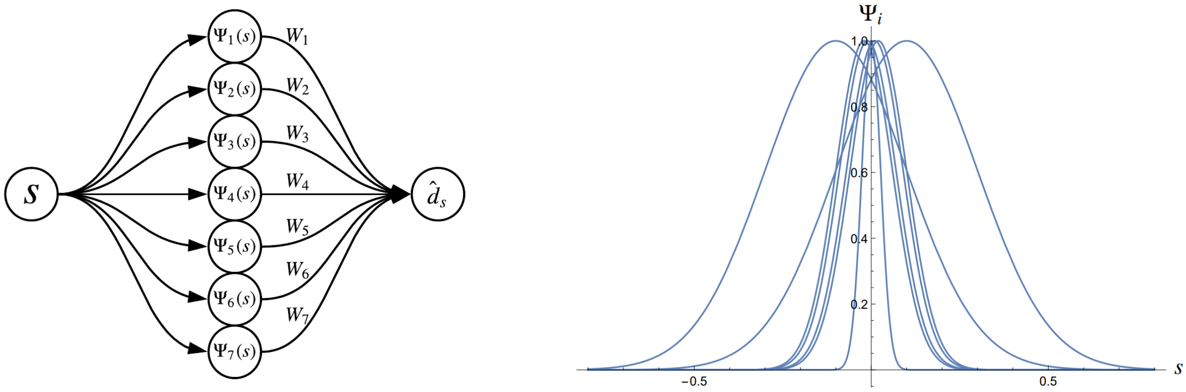

(a) Neural network architecture (b) Activation functions of the neural network

Figure 2: Representation of the RBF neural network

The simulation were executed to verify the influence of the adaptive term in the system's control. It was employed the Runge-Kutta method with the sampling rates of 100Hz for the controller and 200Hz for the system dynamics and the following simulation parameters are considered: $m_1 = 2.16$ kg, $m_2 = 0.494$ kg, $l_1 = 0.05$ m, $l_2 = 0.2$ m, $I_1 = 0.0027$ kgm^2, $I_2 = 0.0016$ kgm^2, and a viscous damping term, $\left[c_1\dot{\theta}_1 \quad c_2\dot{\theta}_2\right]^\top$ with $c_1 = 0.003\ Nms^{-1}$ and $c_2 = 0.001\ Nms^{-1}$, is added to system's model in Eq.(11). Regarding the control parameters, the following values were chosen: $\alpha_a = 0.1$, $\alpha_u = 1$, $\lambda_a = 0.1$, $\lambda_u = 1$, $\phi = 0.4$, $\psi = 0.4$, $\zeta = 0.1$, $\delta = 0.5$, $\eta = 200$, and a 15% error in all simulation parameters. The initial conditions of the system are set to 0° for the rotation base and approximately 23° for the pendulum. Fig. 3 shows the obtained results.

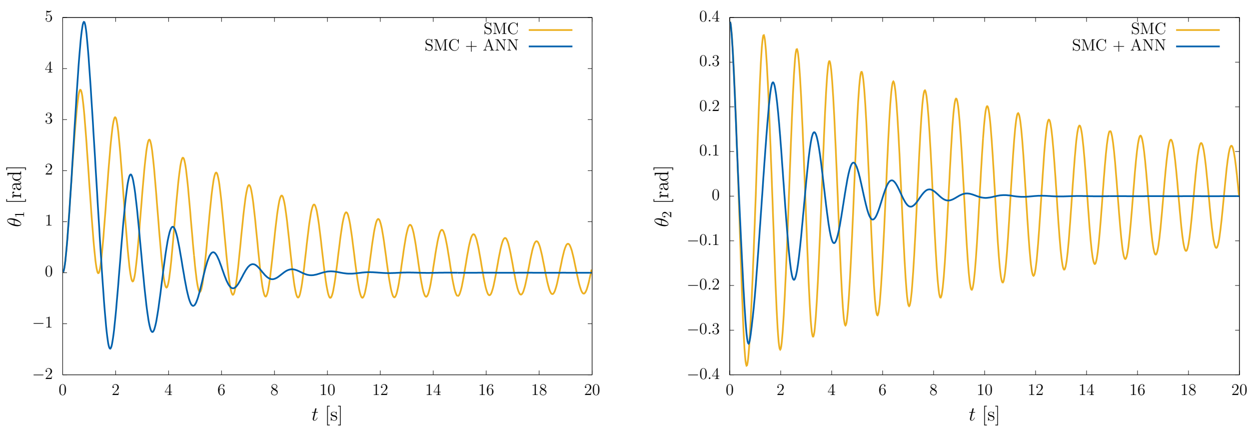

(a) Angular position of the rotating base (b) Angular position of the pendulum

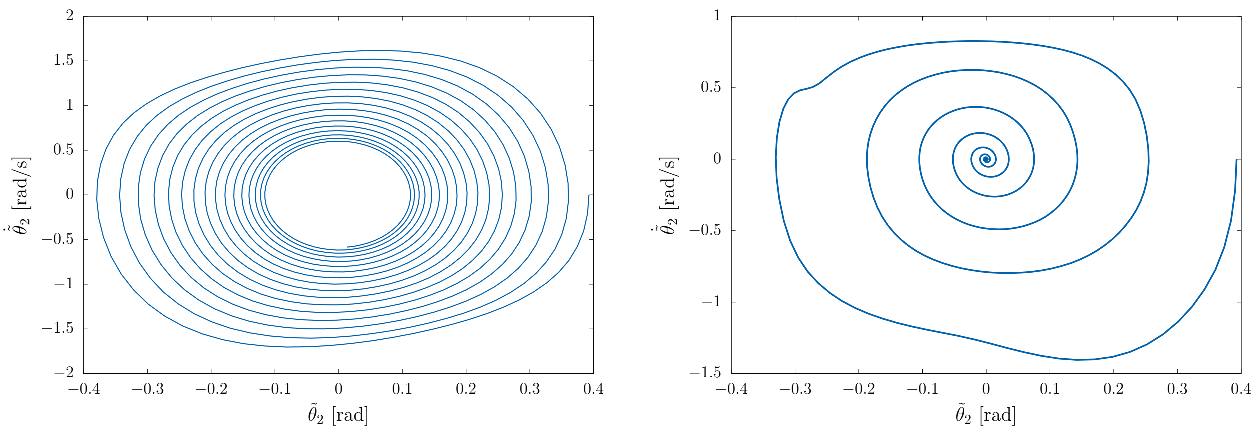

(c) Phase portrait, conventional SMC (d) Phase portrait, SMC+ANN

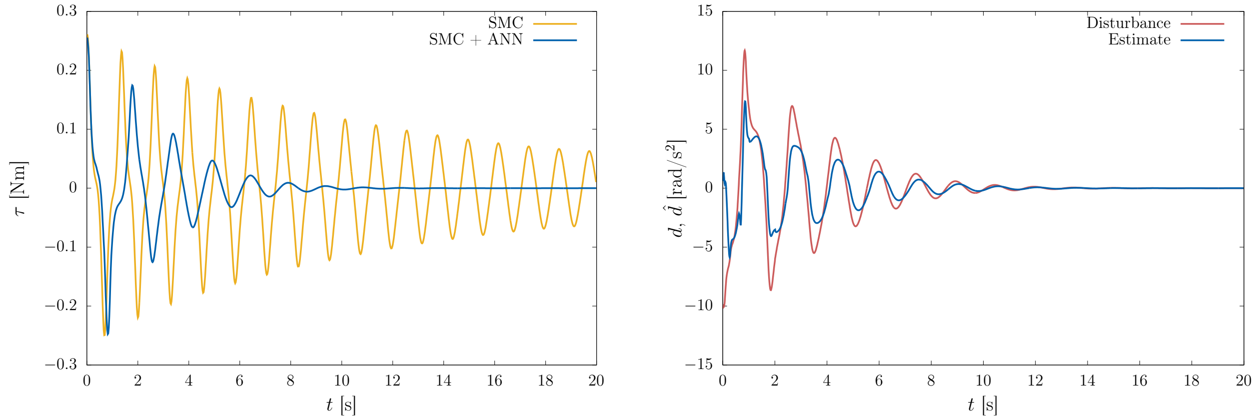

(e) Entry torque applied by the actuator (f) Unmodeled disturbances development

Figure 3: Simulation results for control methodology SMC+ANN

As observed in Fig. 3, there is a great difference in efficacy between the traditional SMC and the SMC+ANN method. Among the benefits, can be cited: reduction in control effort made by the actuator, better stabilization time e decrease in oscillations to an equilibrium point, in addition to a total elimination of the chattering effect.

Also, it is demonstrated in Fig. 3(f) the capacity of the neural network to estimate the system's error. Although the error is not precisely approximated, it is enough for the sliding modes control law, which has a compensator for the parametric uncertainties giving robustness for the controller, to be able to stabilize the system.

CONCLUSION

This work explores the idea of controlling underactuated mechanical systems with a sliding modes controller and artificial neural network methodology. Both convergence and stability properties are proven using the Lyapunov's stability control. The effectiveness of this control law is verified by numerical simulations with results confirming that for underactuated system, the proposed modification to the sliding modes controller is a great form to cope with the uncertainties and dynamic complexity.

ACKNOWLEDGEMENTS

The authors would like to acknowledge the support of the Brazilian Coordination for the Improvement of Higher Education Personnel (CAPES) and of the Federal University of Rio Grande do Norte (UFRN).

REFERENCES

Ashrafiuon, H, Erwin, R.S., 2008, "Sliding mode control of underactuated multibody systems and its application to shape change control", International Journal of Control, Vol.81, No. 12, pp. 1849–1858.

Bessa, W.M., Barrêto, R.S.S., 2010, "Adaptive fuzzy sliding mode control of uncertain nonlinear systems", Controle & Automação, Vol.21, No. 2, pp. 117–126.

Bessa, W.M., De Paula, A.S., Savi, M.A., 2012, "Sliding mode control with adaptive fuzzy dead-zone compensation for uncertain chaotic systems", Nonlinear Dynamics, Vol.70, No. 3, pp. 1989–2001.

Bessa, W.M, et al, 2017, "Design and Adaptive Depth Control of a Micro Diving Agent". Ieee Robotics And Automation Letters, Vol.2, No. 4, pp. 1871-1877.

Bessa, W.M., Kreuzer, E., 2018, "An Intelligent Sliding Mode Control for Underactuated Mechanical Systems". Xxii Congresso Brasileiro de Automática. João Pessoa, Brazil.

Farrel, J.A., Polycarpou, M.M, 2006, "Adaptive Approximation Based Control: Unifying Neural, Fuzzy and Traditional Adaptive Approximation Approaches"", Ed. John Wiley & Sons Inc, Hoboken, EUA, 422 p.

Haykin, S., 2008, "Redes Neurais: Princípios Práticos", Ed. Bookman, Porto Alegre, Brazil, 900 p.

Seifried, R., "Dynamics of Underactuated Multibody Systems: Modeling, Control and Optimal Design, Solid Mechanics and Its Applications", Ed. Springer, 2013.

Seifried, R, Blajer, W., 2013, "Analysis of servo-constraint problems for underactuated multibody systems", Mechanical Sciences, Vol.4, No.1, pp. 113–129.

Slotine, J.E., LI, W., 1991, "Applied Nonlinear Control", Ed. Prentice-hall Inc, Englewood Cliff, EUA, 462 p.

Tanaka, M.C., de Macedo Fernandes, J.M., Bessa, W.M., 2013, "Feedback linearization with fuzzy compensation for uncertain nonlinear systems", International Journal of Computers, Communications & Control, Vol.8, No. 5, pp. 736–743.